CONF-801091--8

Preprint of Paper Presented at

INTERNATIONAL SYMPOSIUM OF FUEL ROD SIMULATORS —
DEVELOPMENT AND APPLICATION

October 22–24, 1980
Gatlinburg, Tennessee

MASTER

DEVELOPMENT OF VARIABLE WIDTH RIBBON HEATING ELEMENTS FOR LIQUID METAL AND GAS-COOLED FAST BREEDER REACTOR FUEL ROD SIMULATORS

R. W. McCulloch D. W. Post
R. T. Lovell S. D. Snyder

Oak Ridge National Laboratory

OAK RIDGE NATIONAL LABORATORY
Oak Ridge, Tennessee 37830
operated by
UNION CARBIDE CORPORATION
for the
DEPARTMENT OF ENERGY

DISCLAIMER

DEVELOPMENT OF VARIABLE WIDTH RIBBON HEATING ELEMENTS FOR LIQUID METAL AND GAS-COOLED FAST BREEDER REACTOR FUEL ROD SIMULATORS*

R. W. McCulloch D. W. Post‡
R. T. Lovell† S. D. Snyder

Oak Ridge National Laboratory
Oak Ridge, Tennessee 37830

ABSTRACT

Variable width ribbon heating elements have been fabricated which provide a chopped cosine, variable heat flux profile for fuel rod simulators used in test loops by the Breeder Reactor Program Thermal Hydraulic Out-of-Reactor Safety test facility and the Gas-Cooled Fast Breeder Reactor Core Flow Test Loop.

Thermal, mechanical, and electrical design considerations result in the derivation of an analytical expression for the ribbon contours. From this, the ribbons are machined and wound on numerically controlled equipment. Postprocessing and inspection results in a wound, variable width ribbon with the precise dimensional, electrical, and mechanical properties needed for use in fuel pin simulators.

---

*Research sponsored by the Office of Research and Technology, U.S. Department of Energy under contract W-7405-eng-26 with the Union Carbide Corporation.

†Fabrication Division, Y-12 Plant, Union Carbide Corporation, Oak Ridge, Tennessee.

‡Development Division, Y-12 Plant, Union Carbide Corporation, Oak Ridge, Tennessee.

INTRODUCTION

Nuclear fuel rod simulators (FRSs or rods) are necessary to the operation of the thermal-hydraulic test facilities for four Oak Ridge National Laboratory (ORNL) programs. These programs and their facilities are the Blowdown Heat Transfer—Thermal Hydraulic Test Facility (BDHT-THTF), the Gas Cooled Fast Reactor—Core Flow Test Loop (GCFR-CFTL), the Breeder Reactor Program—Thermal Hydraulic Out-of-Reactor Safety (BRP-THORS) facility, and the Multirod Burst Test (MRBT) Program and test facility. These experimental facilities are used to conduct out-of-reactor thermal-hydraulic and mechanical interaction safety tests for both light-water and breeder reactor programs. The FRS units simulate the geometry, heat flux profiles, and operational capabilities of a reactor core fuel element under steady-state and transient conditions. The FRSs are subjected to temperatures as high as 1375°C (2500°F) and power levels as high as 57.5 kW/m (17.5 kW/ft), as well as severe thermal stresses during transient tests.

The heat flux profile for an FRS is generated by a tubular or coiled ribbon heating element embedded in boron nitride (BN) insulation within a stainless steel sheath. "Chopped cosine" (cosine profile chopped at either end so that power goes to zero abruptly) heat flux profiles for BRP-THORS and GCFR-CFTL FRSs have been generated by varying the helical pitch of a constant width ribbon. This method, while acceptable for steady-state tests, resulted in unacceptable profile perturbations during transient heat flux. A thorough summary of development in support of the BRP program is presented in Ref. 1.

This paper describes the design, fabrication development, and inspection of variable width, helically wound heating elements, which eliminate the disadvantage of variable pitch ribbons while providing other important advantages to an evolving FRS fabrication technology.

FUEL ROD SIMULATOR

Variable width ribbons were developed for the BRP-THORS and the GCFR-CFTL FRSs. While they are similar in many respects, there are major differences in the purpose, design, and operation of the two simulators. This paper discusses variable width ribbons for the THORS FRS.

The THORS FRS (Fig. 1) is intended for use in a liquid sodium environment. It has a double-ended design (current enters one end and exits the other) with a 5.84-mm-OD (0.230-in.) by 0.38-mm-thick (0.015-in.) clad. The 3.175-mm-OD (0.125-in.) heating element has a total resistance of 3.039 Ω, a peak-to-average heat flux profile of 1.30:1, and a peak-to-minimum profile of 2.92:1. The BN preforms provide structure and insulation in the central and annular regions. Three 0.38-mm-OD (0.015 in.) type K, insulated junction thermocouples, with BN backfilled into the junction region, are located on the clad inside diameter at

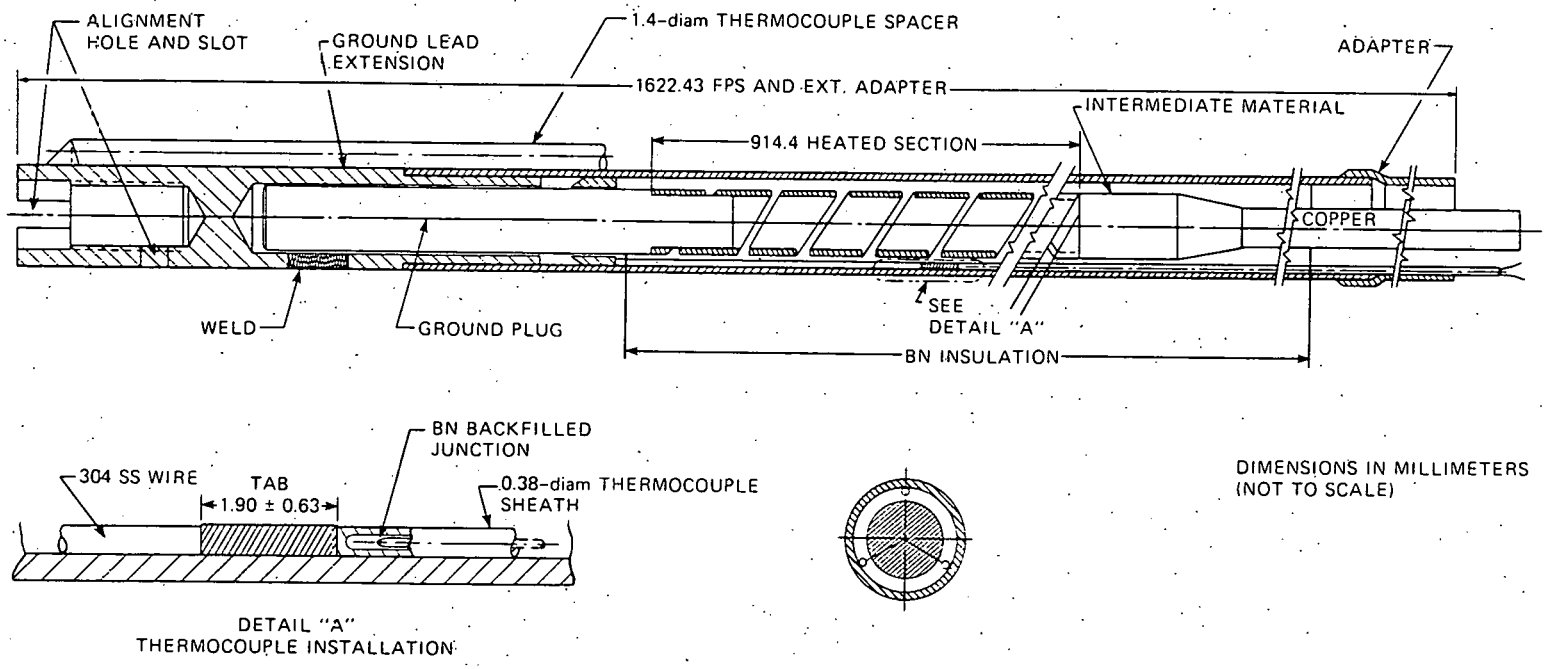

Fig. 1. BRP fuel rod simulator.

120° intervals and various axial locations within the FRS annular region. The variable width ribbon is externally connected to the power supply via a nickel intermediate rod which is in turn joined to a copper rod. The ground connection is made by welding a nickel ground plug to the ground lead extension (Fig. 1).

Power is obtained by I^2R heating of the ribbon. The FRS is capable of operating at 400 W/cm^2 (55.0 kW/m, 390 V at 130 A) at 1000°C (1832°F) clad temperature for short periods of time and at 315 W/cm^2 (43.3 kW/m) at 1000°C indefinitely. Additionally, the FRS is designed to withstand sodium voiding and clad dryout for 1 s while operating at the latter condition. Several core simulations using FRSs have been assembled and tested under various operational conditions in the THORS facility.[2]

DESIGN

For peak FRS performance, the heating element, as the power generating component, is required to operate under conditions approaching the maximum capability of the material. The geometry of, and the configuration within, the FRS must be optimized based upon careful consideration of the thermal, mechanical, and electrical properties of FRS materials for the operational range.

High heat flux FRSs may have a radial temperature profile as high as 260°C/mm so that the radial distance from clad outside diameter to heating element inside diameter directly determines maximum operating conditions for the heating element for a given clad temperature. Generally, the coiled heating element diameter should be as large as possible while maintaining an appropriately thick BN insulation between the heating element and the FRS cladding. This annular region, which contains the FRS internal thermocouples, must maintain acceptable insulation resistivity at the required operational temperatures and must withstand the voltage potential between heating element and clad or thermocouples without dielectric breakdown.

Because FRS peak internal temperature will increase as the ribbon thickness is increased, the thickness of the heating element should be as small as practical. Problems in forming or fabricating the ribbon, as well as handling, assembling, and swaging of ribbons and FRSs, place practical limits on the minimum ribbon thickness. The heating element must be capable of withstanding differential thermal expansion without permanent deformation during transient testing. As the ribbon thickness decreases, the percent variation in thickness becomes much harder to control. This in turn affects local heat generation, because local power generation (with constant current through the ribbon) is inversely proportional to thickness. A practical ribbon thickness and tolerance limit is 0.25 ± 0.0125 mm (0.010 ± 0.0005 in.).

Because transient operation of the FRS is of paramount concern, the heating element configuration must be carefully analyzed under transient conditions as part of the design effort. Heat capacity effects become

pronounced in the transient heat flux profile, and axial and circumferential conduction do not smooth out the profile as they do under steady-state conditions. Furthermore, with the use of BN preform technology, axial conduction is much lower than radial conduction because of the anisotropic nature of thermal conductivity in BN preforms. Thus, under transient conditions, such properties as the turn-to-turn spacing, ratio of coil surface area to sheath surface area, coil diameter variation, coil turns per unit length, and eccentricity of the heating element become important.

Evaluation of thermal, mechanical, and physical properties of the heating element material provide design limits for the variable width coil and assure that it can be fabricated and will be suitable to its environment. Electrical considerations provide the design basis for the exact configuration to meet FRS operating requirements.

Design of the heating element is dependent upon current and voltage available from the power supply. For parallel connection of the FRS to the power supply, a heating element resistance "window" can be calculated by

$$R_{max} = V^2/P \ , \tag{1a}$$

$$R_{min} = P/I^2 \ , \tag{1b}$$

where V is voltage, P is power in watts, and I is current. Factors such as terminal I^2R heating, large bundle connection, FRS dielectric breakdown, and material temperature coefficient of resistance (TCR) must also be considered in optimizing the element resistance.

Once the resistance has been determined, the design of a constant width, rectangular ribbon heating element can be accomplished using the method illustrated in Fig. 2. From this, ribbon width w is derived in terms of the physical and dimensional parameters of the heating element:[1]

$$w = \left(\frac{\pi D \rho C}{Rt}\right)^{1/2} . \tag{2}$$

The ribbion thickness t, coil pitch diameter D = OD − t, material resistivity ρ, wound element resistance R, and axial heated length C are the input parameters that, along with the ribbon width w, completely define the wound coil.

Once the width has been determined, factors describing the FRS power profile are needed. These are peak/average power, P_p/P_a; peak/minimum power, P_p/P_m; and coil axial length C. Figure 3 shows a typical chopped cosine profile where P_p, P_a, P_m, and C are defined.

The power profile of Fig. 3 can be defined by

$$P = P_p \cos \phi \ , \tag{3}$$

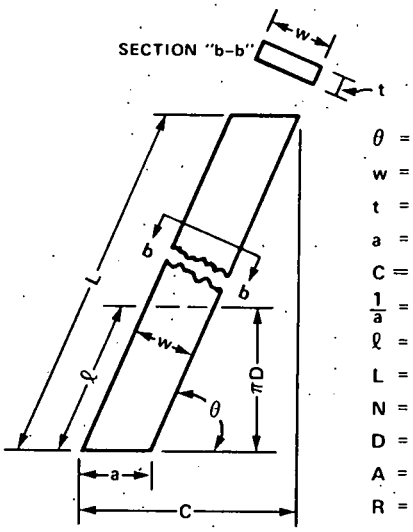

DEFINITIONS

θ = WINDING ANGLE
w = WIDTH OF HEATING ELEMENT
t = THICKNESS OF HEATING ELEMENT
a = AXIAL LENGTH OF WIDTH
C = AXIAL LENGTH OF HEATING ELEMENT
$\frac{1}{a}$ = TURNS PER CENTIMETER
ℓ = LENGTH OF RIBBON FOR 1 TURN
L = OVERALL LENGTH OF RIBBON
N = NUMBER OF TURNS IN COIL
D = PITCH DIAMETER OF COIL
A = CROSS-SECTIONAL AREA OF RIBBON
R = RESISTANCE OF HEATING ELEMENT

DERIVATIONS

$$\sin\theta = \frac{\pi D}{\ell} = \frac{w}{a},\ \cos\theta = \frac{a}{\ell} = \frac{w}{\pi D},$$

$$N = \frac{C}{a} = \frac{C\sin\theta}{w} = \frac{C}{\pi D}\tan\theta,\ L = N\ell = \frac{C}{\cos\theta},$$

$$A = \frac{\rho L}{R} = \frac{\pi D\,\rho\,C}{R\,w},\ \text{SO}\ w = \frac{A}{t} = \left(\frac{\pi D\,\rho\,C}{R\,t}\right)^{1/2}$$

Fig. 2. Considerations of winding a ribbon of length L on a pitch diameter D for an axial length C results in an equation that defines ribbon width in terms of the material and dimensional properties.

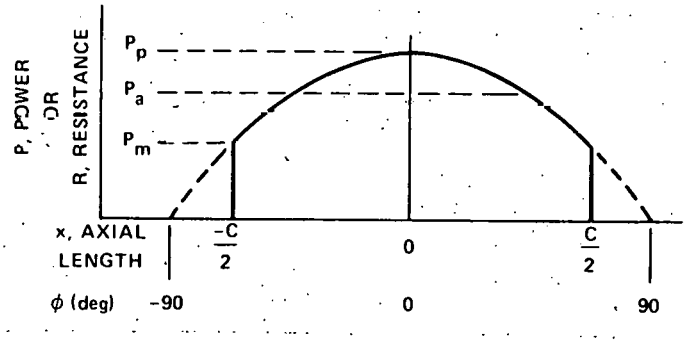

Fig. 3. Variable heat flux chopped cosine profile.

where ϕ is the angle that relates the power profile to the coil axial length C. By definition, $\cos \phi_p = P_p/P_p = 1$, and $\phi_p = 0°$ at P_p. The angle at P_m where $x = \pm C/2$ is now

$$\phi_m = \cos^{-1} (P_m/P_p) . \tag{4}$$

The profile can now be described within the "chopped region" by

$$P = P_p \cos \phi = P_p \cos \left[\frac{2x}{C} \cos^{-1} (P_m/P_p)\right] . \tag{5}$$

Equation (5) relates the chopped cosine profile analytically to the axial power variation.

Since current is constant through the heating element, power is proportional to resistance. The local peak resistance R_p is in the center of the profile and is given by

$$R_p = \frac{R}{C} \cdot \left(\frac{P_p}{P_a}\right) , \tag{6}$$

as shown in Fig. 3.

The ribbon width at the peak of the profile, w_p, (where $P = P_p$) can now be calculated from Eq. (2) by replacing R with R_p of Eq. (6) and taking C to be of unit length:

$$w_p = \left(\frac{\pi D \rho}{R_p t}\right)^{1/2} . \tag{7}$$

The design of a ribbon profile to give a specific axial heat flux distribution was first reported by D. L. Clark and T. S. Kress.[2] The local heat flux distribution was established by them to be:

$$P = \frac{I^2 \rho}{w^2 t} , \tag{8}$$

where P is the local power per unit area, w is the local ribbon width, and I is the current.

From Eq. (8), the local ribbon width w is

$$w = \left(\frac{I^2 \rho}{P t}\right)^{1/2} . \tag{9}$$

If Eq. (9) defines the power at some reference position such as the center where $P = P_p$ and $w = w_p$ (Fig. 3), then the local width w, with respect to the reference width, is

$$w = \left(\frac{P_p}{P}\right)^{1/2} w_p \ . \tag{10}$$

Equation (10) can be used to establish the relative width anywhere along the ribbon. However, knowing just the width is not sufficient. The ribbon must be wrapped around a mandrel to form the coil of the desired diameter and length L. Figure 4 shows the uncoiled ribbon contour and the coiled configuration. For the coil to wind properly, the vertical contour angle θ must be the same on both sides of the ribbon at any position along the abcissa shown in Fig. 4. Thus, for the gap $G_v = 0$, the vertical component of the width of the ribbon, w_v, is constant and is

$$w_v = \pi D \ , \tag{11}$$

where D is the ribbon pitch diameter as defined previously. The local width w is given in terms of the contour angle θ by

$$w = \pi D \cos \theta \tag{12}$$

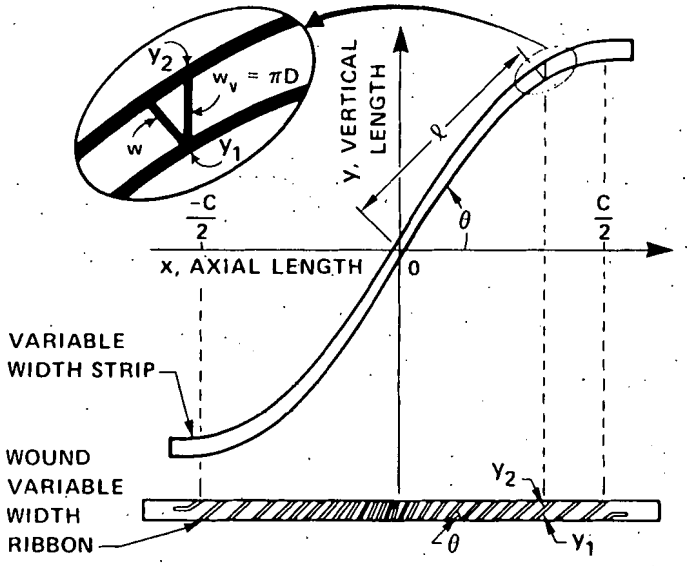

Fig. 4. Variable width contour is designed with a constant vertical width, $W_v = \pi D$. Local width W varies with winding angle θ to allow coil to be wound on a circumference πD with no variation in gap between turns.

or in terms of a reference angle θ_p at P_p, w_p by

$$\cos \theta = \left(\frac{P_p}{P}\right)^{1/2} \cos \theta_p \ . \tag{13}$$

The vertical contour or winding angle, θ, can now be determined in terms of the specific profile information by substitution of Eq. (5) into Eq. (13):

$$\cos \theta = \left\{ \frac{1}{\cos\left[(\cos^{-1} P_m/P_p)\ \frac{2x}{C}\right]} \right\}^{1/2} \cos \theta_p \ . \tag{14}$$

Then local width w is calculated using Eq. (12). This defines the ribbon contour in terms of θ and w at any axial length x for $-C/2 \leq x \leq C/2$.

The final task is then to determine the ribbon length ℓ and the vertical length y in terms of x for a given ribbon contour and to compile the information in a form that can be used to generate magnetic tapes for machining and winding the ribbons.

From Fig. 4:

$$\ell = \frac{x}{\cos \theta} \ , \tag{15}$$

and

$$y = x \tan \theta \ , \tag{16}$$

where ℓ is the length of one turn. Equations (14), (12), (15), and (16) completely define the parameters of a variable width ribbon in terms of the axial length x. These data, computed from a programmable calculator, are then used as input to generate ribbon machining and winding control tapes.

MACHINING

The objective of the machining phase of ribbon development is to convert the ribbon contour information into ribbons of variable width that have a precisely controlled contour. The major requirements are to hold the width variation and the x and y locations describing the ribbon

contour on the x-y plane (and therefore the angle) to within 1% throughout the ribbon length.

Early attempts to machine the ribbon contour on a numerically controlled (NC) horizontal milling machine were unsuccessful because these tolerances could not be held, excessive ribbon edge burring occurred, and machine time per ribbon was excessive.

These difficulties prompted investigation of the use of grinding techniques which allowed machining (grinding) a stack of elements simultaneously. This method eliminated edge burrs and reduced fabrication time. Dimensional inaccuracies were overcome by using a high precision NC template grinding machine (Fig. 5), which is equipped with a 50.8-cm-diam (20-in.) rotating oscillating aluminum oxide grinding wheel with an adjustable vertical oscillating stroke, mounted on the "Y" axis or main slide. It has been retrofitted with a vertical milling attachment that is mounted on the grinding wheel housing. However, the "X" axis or cross slide machine travel was only about two-thirds as long as was needed to machine current ribbon designs. This limitation was overcome by using a staging technique to effectively extend the cross slide travel from 137 cm (54 in.) to ~245 cm (96.5 in.). Thus, slide travel was provided to machine the element contour of all design configurations of interest.

Ribbons are machined from strips of base stock up to 15.2 cm (6 in.) in width and 259.1 cm (102 in.) in length; up to 15 of these

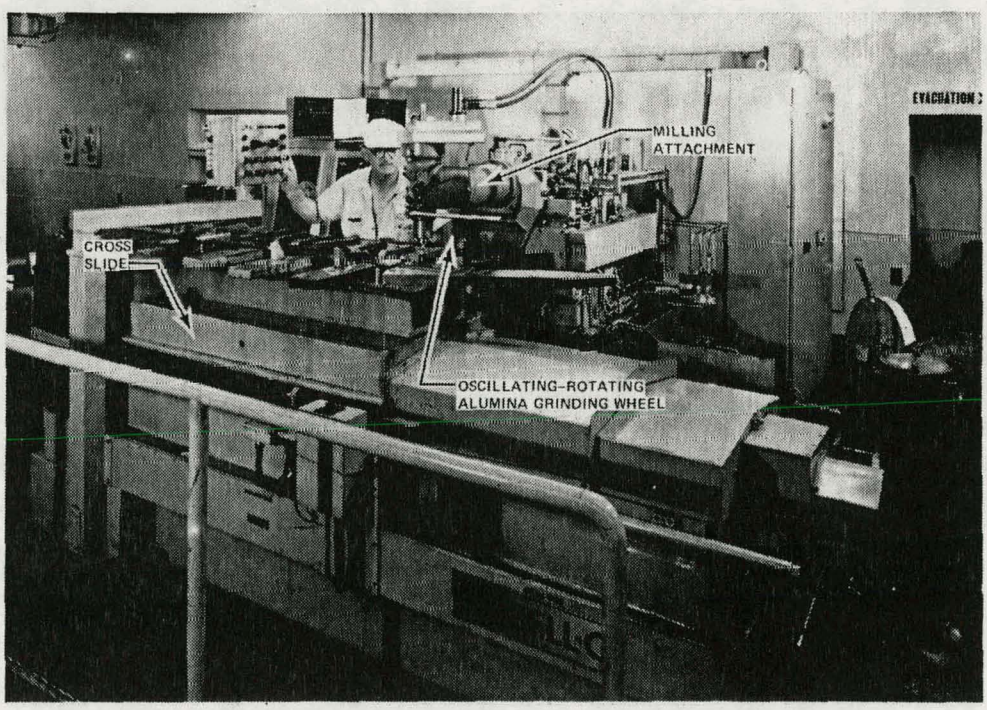

Fig. 5. Numerically controlled template grinding machine.

strips are stacked together and clamped between steel plates. Figure 6 shows the heating element geometry within the base stock.

As the figure shows, up to 5 sets of 15 ribbons can be obtained from one stock assembly. The machining sequence is as follows:

1. The upper left surface of stack one is machined.
2. The upper right surface of stack one is machined.
3. The stack is reversed and remounted on the machine.
4. The region between stacks one and two is milled and the first stack of 15 strips is separated from the rest of the assembly.
5. The upper left surface of the first stack is completed.
6. The upper right surface of the first stack is then machined, completing the first stack.

Stacks 2 through 5 are completed similarly.

A typical ribbon machining operation uses two numerically controlled drive tapes (designated as stages one and two in Fig. 6) generated from the design calculations. The first stage tape is designed to control more than half of the element contour machining. At the end of the program, an angular tab is defined to establish the relationship of the second stage tape to the program of the first stage tape. The path defined by the stage one program and its relation to the stage two program are shown in Fig. 7. As shown, the program travel of the second

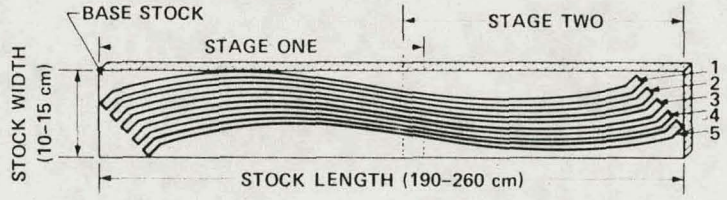

Fig. 6. Fuel pin simulator heating element geometry within ribbon stock.

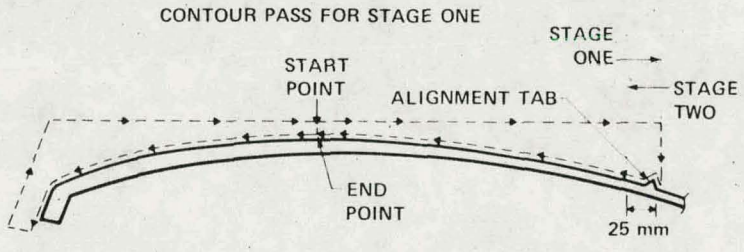

Fig. 7. Stage one contour machining. Pass starts at high point at (1), proceeds down, then left to ribbon end, moves up, then longitudinally to alignment tab, and completes contour pass adjacent to starting point. Stages one and two overlap at the alignment tab by 25 min.

stage tape overlaps the programmed travel of the first stage tape by ~25 mm (1 in.) so that the tool path of the second tape will blend with the finished surface of the first tape. These two tapes control (1) the end mill operation that separates the five stacks of material and (2) the grinding of the full contour of one side of a variable width ribbon. Fixturing enables the ribbon stack to be removed and reversed so that the other (symmetrical) side can be machined.

With the entire stack clamped in position on the front side support fixture, which is mounted on the cross slide of the machine, the first stage of the front side of the element is rough machined using the end mill attachment. After the end milling pass is completed, the milling spindle is replaced by the grinding wheel; and, using the same drive tape as was used for rough milling, the first stage of the element contour is ground to the proper configuration (Fig. 8).

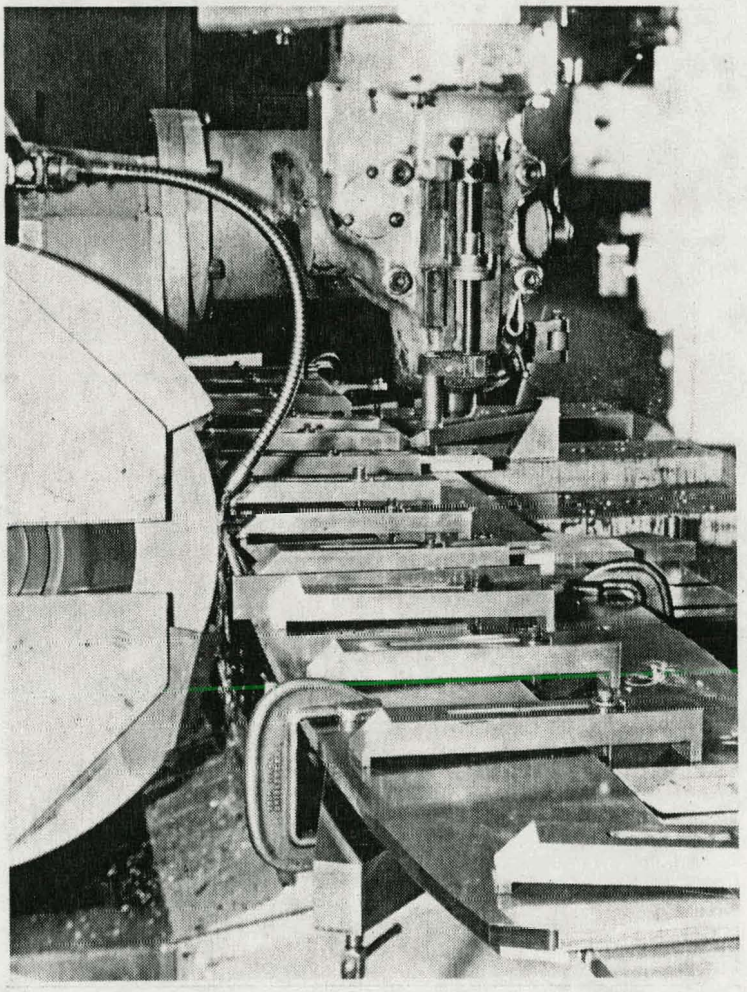

Fig. 8. Finish grinding of first stage of one side of heating element.

Still encased in the support fixture, the assembly is then moved longitudinally on the cross slide, and the milling spindle is brought back into position for rough milling the second stage of the front side contour. Alignment of the stage two contour pass to that of stage one is maintained by positioning the end mill on the two surfaces of the tab at the end of the stage one contour (Fig. 9). After completion of the stage two milling, the milling spindle is again replaced by the grinding wheel and the contour is finish ground.

At this point in the machining process, the element stack–fixture assembly is removed from the machine, and the first fixture is replaced with a backup plate fixture which is then aligned on the cross slide. This second fixture consists of a top and bottom support plate attached

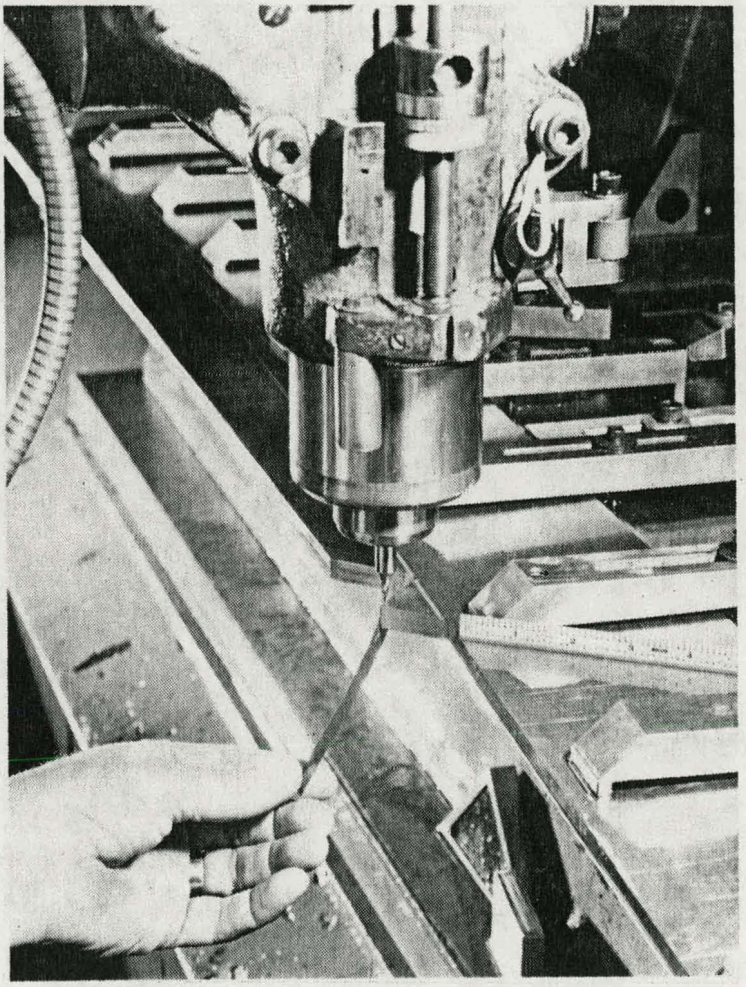

Fig. 9. Alignment of stage two contour to that of stage one as maintained by positioning end mill on tab surfaces.

to an auxiliary support fixture by an attachment bar (Fig. 10). After alignment, the element stack–fixture assembly is positioned so that the previously finished front side contour is firmly placed against the premachined contour of the backup plate. This establishes a reference surface between the two sides of the ribbon stock.

With the element stack nestled in the backup plate fixture and supported by the auxiliary support fixture, stage one of the second side of the element contour is separated from the stack by an end mill operation. After the stage one milling is completed, the entire assembly is moved on the cross slide into position and stage two of the contour is end milled (Fig. 11). This first element is now separated from the remainder of the stack (Fig. 12). The auxiliary support fixture is then removed from the machine, and the backup plate fixture with the elements attached is repositioned on the cross slide. The second side contour is now ready for first stage finish grinding.

The second side of the element contour is ground in a manner similar to the first side contour, with the final relationship between the

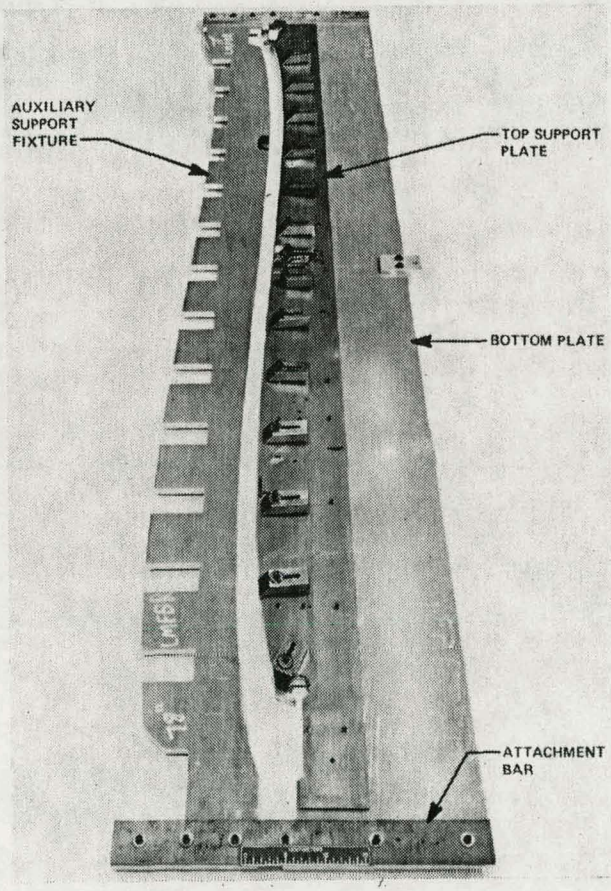

Fig. 10. Backup plate fixture and auxiliary support fixture attached to each other by attachment bars at either end.

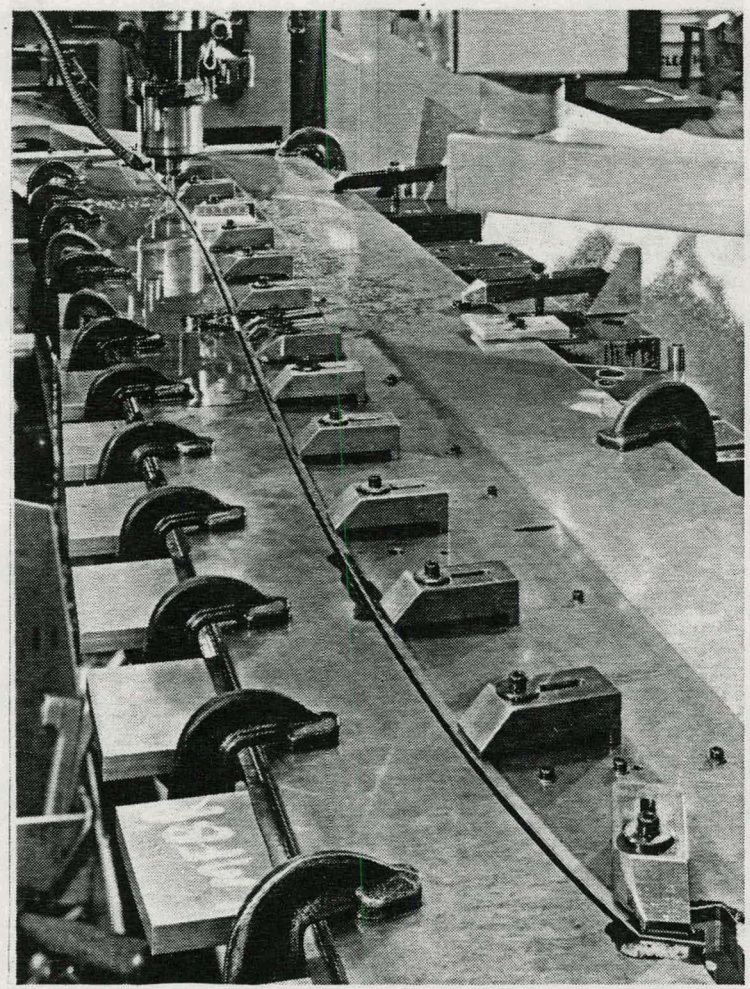

Fig. 11. End milling of second side ribbon contour.

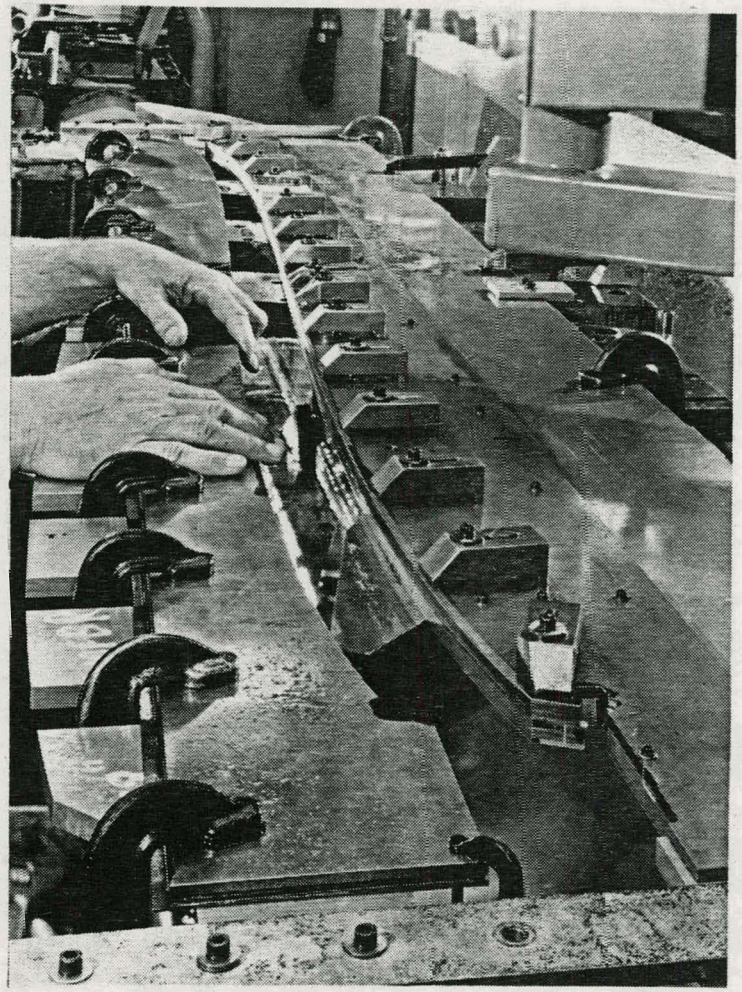

Fig. 12. After completion of stage one and two milling passes on second side, element stock is separated from the rest of the stock.

first and second stages being controlled by width measurements taken at the midpoint and the ends of the element (Fig. 13). When the design width of the element has been reached at the blend point of the first and second stages, the machining of the stack of 15 elements is completed. Four additional groups are then machined for a total of 75 ribbons. Local width and contour tolerances of 0.013 mm (0.0005 in.) are consistently achieved.

WINDING

The variable width ribbons are formed into spirally wound coils on a stainless steel mandrel by a high-precision automated winding machine.

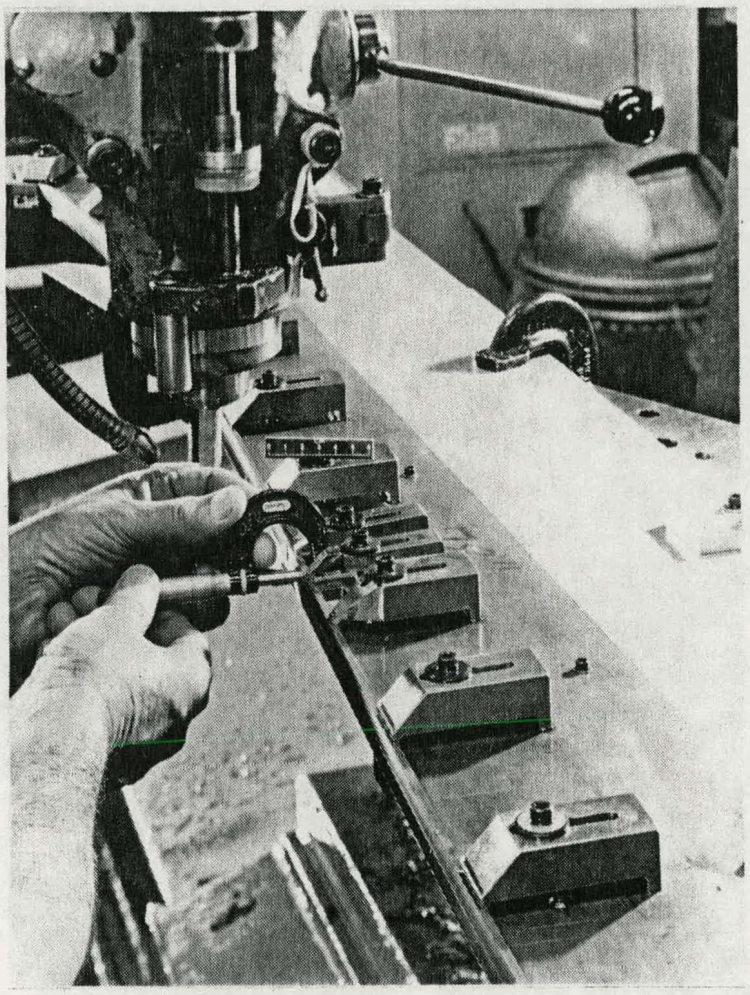

Fig. 13. Final contour width tolerances are obtained by width measurements at center and ends of element stock.

To obtain reproducibility of coil parameters, the winding equipment must have a controllable variable lead rate (centimeters per/revolution). This lead rate must be programmed to maintain a variable vertical speed defined by the variation in ribbon width at points along the ribbon contour. Rotational velocity remains constant throughout the process.

The Black-Clawson four-axis NC winding machine, depicted schematically in Fig. 14, was selected to fabricate the coils. Only the "Y" axis and the "θ" axis motions are required for winding.

A typical coil winding operation uses an appropriately sized stainless steel rod loaded under tension between the headstock (machine base) and the tailstock. With a winding die attached to the machine ram, the headstock rotates as the ribbon is fed into the winding die. The die is advanced by the ram in a controlled vertical movement. Figure 15 depicts the machine in operation, and Fig. 16 provides a close up of the headstock chuck and the coil winding die affixed to the machine ram.

The ribbon is positioned by the ram so that the winding mandrel is concentric to a precision ground hole through the body of the die. The

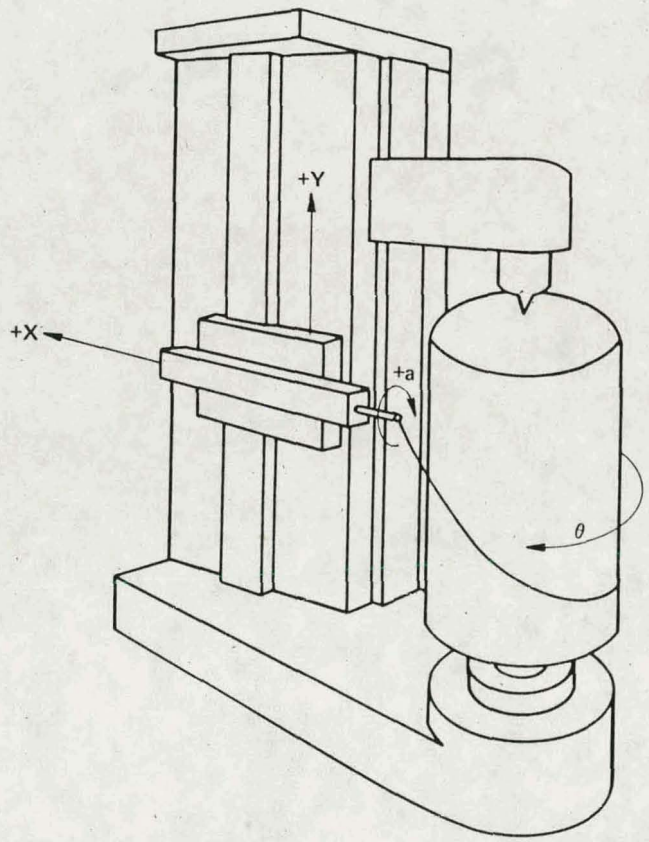

Fig. 14. Schematic layout of Black-Clawson winding machine.

Fig. 15. A variable width ribbon being wound into a coil. Inset shows how ribbon is formed on rotating mandrel by the die.

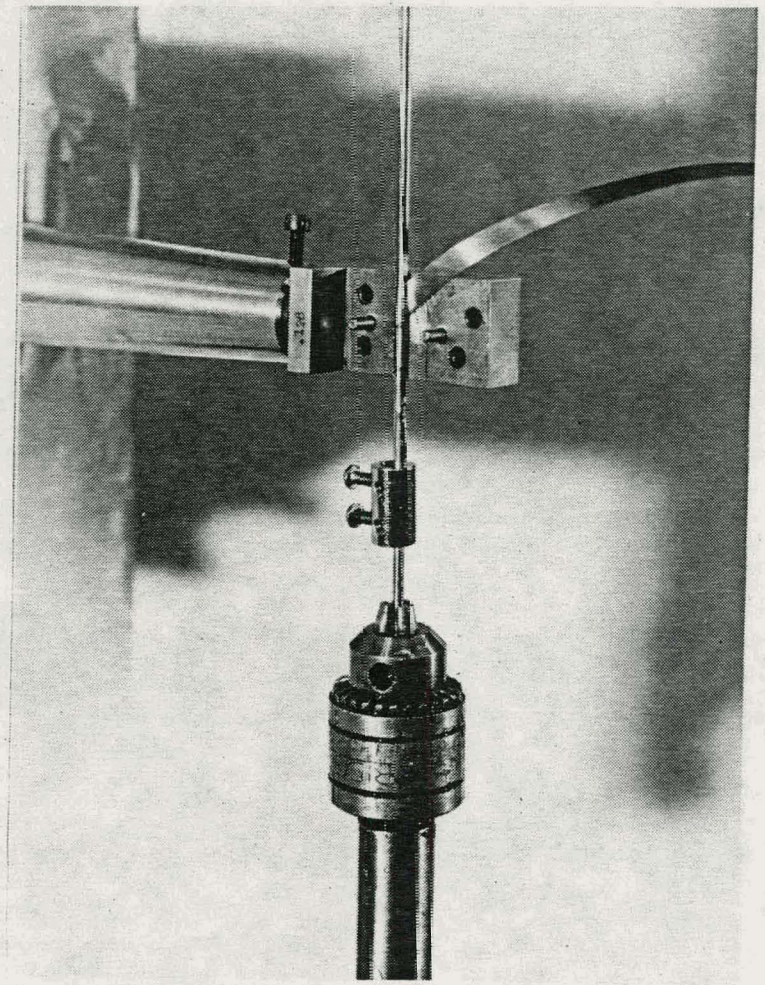

Fig. 16. Headstock chuck and winding die.

die is made in two sections (Fig. 17) so that the ribbons can be positioned at the correct feed angle prior to initiation of the automatic winding cycle. The forming area of the die is made of tungsten carbide to reduce spalling and ribbon damage.

Figure 18 shows the hand tool used to form the lead tab of the ribbon in preparation for attachment to the mandrel. The first two coil turns are manually wound on the mandrel (Fig. 16), and the mating half of the winding die is then attached. A ribbon strip feed slot with a feed angle at 22.5° is machined on one-half of the die body. This slot is required to allow the ribbon to feed freely into the working bore of the die; it also automatically maintains the proper feed angle at the coil midpoint.

Coils can be easily wound with diameter uniformity of 0.125 mm (0.005 in.) and length (as well as gap) tolerance variations of about 5%. Coils with these tolerances are more than sufficient for use in FRSs because they receive a final swaging operation before installation into the FRS. The swaging operation is described in the next section.

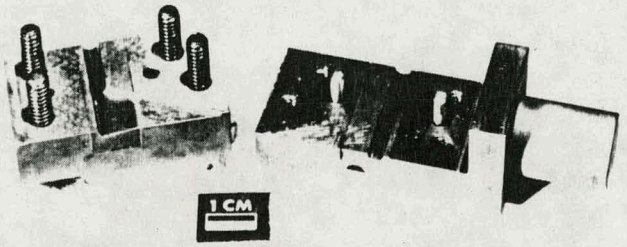

Fig. 17. Ribbon winding die showing ribbon feed region and carbide inserts in forming region.

Fig. 18. Hand tool used to form ribbon lead tab in preparation for attachment to mandrel.

SWAGING AND INSPECTION

A final processing step, swaging, sets the coils to final dimensions and to required tolerances prior to installation of the coils in the FRS.

First, the coils are tightly wound on a hard, stainless steel mandrel with the turns touching. Both ends are attached to the mandrel, one with a clamp and the other by spot welding. The coil is then carefully swaged to lock it into this configuration. After swaging, it is removed from the mandrel. Swaging supplies coldwork to the coil to lock the turns in place, sets the required diameter, removes the concavity introduced by winding, and decreases the surface roughness.

Additional coldwork put into the coils by swaging makes them rigid and mechanically similar to a spring. Then, gaps between turns are produced by stretching the coil about 5% of its length. The coil does not plastically deform under these conditions; thus, the gaps between turns no longer depend on the local material yield stress and are quite uniform. The coil outside diameter can be controlled to within ±0.013 mm (0.0005 in.) using this method.

Coils are dimensionally inspected with a micrometer, cleaned in a vapor degreaser, and cut to the exact length after swaging. To maintain a symmetrical chopped cosine profile, equal amounts of material are cut off each end.

Infrared scanning techniques were used to evaluate how well the heat flux distribution produced by the coils fits the design criteria. Infrared scanning of FRSs has been used for some time at ORNL.[3] As part of this effort, these techniques were extended to relate heat flux perturbations to bare coil dimensional variations and to determine the effect of these variations on the completed FRS heat flux profile.

The most acceptable technique for coil evaluation is (1) to paint the coil with a black paint (to increase surface emissivity), (2) to insert a close-fitting insulated arbor into the center, (3) to stretch the coil on the arbor about 2% of its length, and (4) to scan it after applying a power of about 25 W for 4 min. Much more sensitive analysis of coils is possible by using higher power, shorter time scans, and/or by close, narrow range scans. The 25-W, 4-min scan of a bare coil was determined to be comparable to the 1-s core transient infrared scan commonly used in FRS inspections. These inspections indicate that coil outside diameter variations of ±0.025 mm (±0.001 in.) and coil gap variations of 0.05 mm (0.002 in.) are acceptable from a thermal profile standpoint.

Figure 19 compares infrared scans of a bare coil with the same coil in a completed FRS. A discontinuity in the coil turns causing an abrupt change of about 8% in the center of a heat flux profile is evident in both scans. Figure 20 shows the core steady-state and transient scans and the clad transient scans of a completed BRP FRS with a variable width heating element. The core transient profile is a close replica of the steady-state profile (except for axial conduction at either end).

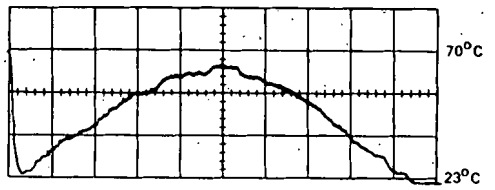

(a) BARE COIL, STRETCHED AND PAINTED; POWERED AT 25 W FOR 4 min

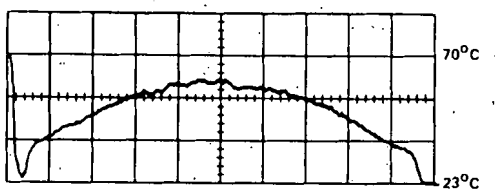

(b) CORE TRANSIENT SCAN OF THE COIL IN (a), INSTALLED IN A FPS; POWERED AT 12.8 kW FOR 1 s

Fig. 19. (a) Bare coil, stretched and printed; powered at 25 W for 4 min. (b) Core transient scan of coil in (a) in an FPS powered at 12.8 kW for 1 s.

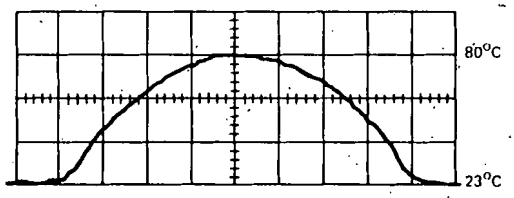

(a) CORE STEADY-STATE TEST; POWERED AT 32 W FOR 4 min

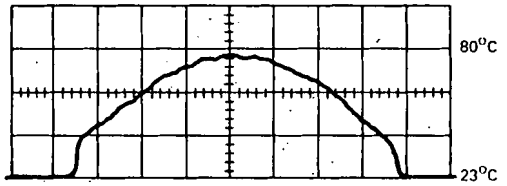

(b) CORE TRANSIENT TEST; POWERED AT 4 kW FOR 1 s

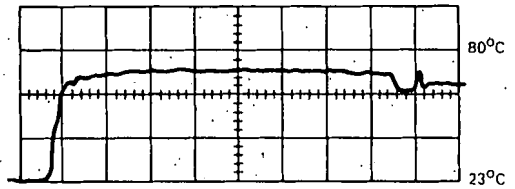

(c) CLAD TRANSIENT TEST; POWERED AT ~4 kW FOR 1 s

Fig. 20. Core steady state (a), core transient (b), and clad transient (c) infrared scans of a completed FRS with chopped cosine variable width ribbon heating element.

Maximum deviation is within 2.5%. Heat flux profiles during transient operation are acceptable with this amount of deviation.

CONCLUSION

Design of variable width ribbon heating elements is based upon a mathematically derived equation for the chopped cosine profile and takes into account the syncronous variation of the local ribbon width with the winding angle so that the cross section (and therefore local heat generation) can change essentially independently of the turn-to-turn spacing.

The ribbon profile, once determined, is machined on a numerically controlled template grinding machine to width and contour tolerances of better than 0.5%. The ribbons are wound into coils using a filament winding machine. The coils are then swaged, cleaned, cut to length, dimensionally inspected, and infrared scanned prior to use.

The elements have been successfully operated as components of THORS Bundle 9 FRS, THORS Bundle 12 FRS prototypes, and GCFR-CFTL Bundle AG-1 FRS prototypes. The coils are fabricated with very small gaps between turns while maintaining a variable profile. These coils have been successfully installed in sophisticated FRSs using precise FRS fabrication technology. This technology includes the use of cold pressed BN preforms as insulation between the heating element and the cladding.

REFERENCES

1. W. E. Baucum, R. E. MacPherson, D. L. Clark, and R. W. McCulloch, *State of the Art Fuel Pin Simulators for LMFBR Out-of-Reactor Safety Tests – Status Report*, ORNL/TM-5889 (September 1977).

2. D. L. Clark and T. S. Kress, U.S. Patent No. 3,912,908, *Electric Cartridge-Type Heater for Producing a Given Non-Uniform Axial Power Distribution*, Oct. 14, 1975.

3. W. A. Simpson, Jr., S. D. Snyder, and K. V. Cook, *Infrared Inspection and Characterization of Fuel-Pin Simulators*, ORNL/NUREG/TM-55 (November 1976).